PRELIMINARY STUDY ON A NOVEL TRANSCRITICAL CO_2 HIGH-TEMPERATURE HEAT PUMP

Ji Wang [a]*, Martin Belusko [a], Ming Liu [a], Michael Evans [b], Alemu Alemu [c], Frank Bruno [a]

[a] Future Industries Institute, University of South Australia, Mawson Lakes Campus, Mawson Lakes SA 5095, Australia

[b] UniSA STEM, University of South Australia, Mawson Lakes Campus, Mawson Lakes SA 5095, Australia

[c] Glaciem Cooling Technologies, Mawson Lakes Boulevard, Mawson Lakes SA 5095, Australia

***Corresponding Author:** Ji.wang@mymail.unisa.edu.au; Jayqinghome@hotmail.com (J. Wang)

ABSTRACT

Carbon dioxide (CO_2), also known as R744, is one of the natural substances, which is an environmentally benign, safe and economical refrigerant used for cooling and heating systems. The transcritical CO_2 heat pump water heater has attracted much attention from researchers in recent years, due to that the CO_2 water heater can contribute to a significant reduction in energy consumption. The CO_2 heat pump system can provide hot water with higher efficiency compared to a traditional electric or gas water heater and can achieve a higher delivery temperature compared to other water heat pumps. Based on existing studies, limited research has considered using the transcritical component of CO_2 to deliver a high enough temperature suitable for high-temperature water/steam production. Although an upper-temperature limit exists in current CO_2 systems, combining this with an electrically driven auxiliary heater can deliver a low-cost steam/water production solution, which can be one of the promising technologies for industrial process heating demand.

The present study aims to address the limitations of existing CO_2 technology by operating an auxiliary heater and employing an internal heat exchanger for further increasing discharge temperature and heat capacity. Four thermodynamic cycles have been identified and investigated with the consideration of industrial applicability. The numerical analysis for a transcritical CO_2 heat pump with the auxiliary heater has been carried out. Several preliminary results with different discharge pressures are described. The results show that the total efficiency of the system will slightly increase with the discharge pressure if the targeted discharge temperature is fixed, and the results of energy distribution show that the ratio of auxiliary heating power to CO_2 heating power decreases with the discharge pressure. Additionally, the mathematical model for Bitzer semi-reciprocating compressors is validated against the experimental data with acceptable agreements.

1 INTRODUCTION

Due to the advantages of energy-saving, high-efficiency and cost-effectiveness, heat pump systems have attracted a lot of attention from researchers recently, and even some of them have been widely used in both residential and industrial sectors (Kim, Pettersen & Bullard 2004). Statistical analysis regarding the heat pump systems across European countries has been conducted by Nellissen et. al (Nellissen & Wolf 2015), which shows the industrial energy usage with different temperatures and the distribution of heat demand from existing heat pumps, i.e. more than half the amount of energy in Europe is currently used for low-temperature heating (below 80°C) while only 43% amount of heat is exploited for high-temperature heating (from 80°C to 150°C).

An international agreement: The Montreal Protocol, decreed to phase out the production of synthetic substances (CFCs, HCFCs) from 1991 and phase down the import of HFCs from 2019 (Velders et al. 2007), as the environmental issues (greenhouse effect and ozonosphere depletion), have been deteriorated due to impacts of synthetic chemicals (Nekså 2002). A range of natural refrigerants then has been considered to replace synthetic refrigerants in the vapour-compression systems (Bamigbetan et al. 2017). Up to now, the most widespread natural refrigerants used in the systems including carbon dioxide, propane, butane, iso-butane, propylene and ammonia (Chaichana, Aye & Charters 2003). CO_2, also known as R744, is a promising refrigerant with an ODP of zero and a GWP of one, which is only inferior to ammonia (Lorentzen 1994). But while the safety factor is considered, i.e. CO_2 is non-explosive and non-toxic but ammonia is both poisonous and flammable (Maina & Huan

2015). Additionally, the price of CO_2 refrigerant per unit mass is around three times cheaper than HFC blends (R404A and R407A) (Bruno, Belusko & Halawa 2019).

According to data released by the Australian government in 2012, the energy consumed for heating water accounts for around 21% of total energy, which produces around 23% of green gas emissions (Chris Riedy 2013). Compared to the electric water heater and gas water heater, a CO_2 heat pump water heater can contribute to a significant reduction in energy consumption and is able to provide hot water with a relatively high COP (Hepbasli & Kalinci 2009). In regards to the current CO_2 water heaters, it has been investigated by researchers for various purposes of potable water heating (Saikawa & Koyama 2016), sanitary water heating (Tammaro et al. 2017), general water heating (Qi et al. 2013), and high-temperature water heating (White et al. 2002). Also, CO_2 heat pump systems with the combinations of water heating and space heating have been developed and investigated (Stene 2005).

The reciprocating compressors are normally selected for current CO_2 heat pump systems because of their higher compression ratio and better efficiency, compared with turbo and scroll compressors (Kus & Nekså 2013), (Zheng et al. 2020). However, due to the upper temperature and pressure limits of current CO_2 reciprocating compressors (140°C and 140 bar for long-term operation), there is limited research focusing on a CO_2 high-temperature heat pump with a heat delivery temperature above 100°C. Therefore, the objective of this study is to investigate a method for achieving a high-enough CO_2 discharge temperature and generating sufficient heat capacity with the consideration of real component constraints. The present study aims to address the limitations by operating an electrically driven auxiliary heater and employing an IHX to deliver a low-cost steam/water production solution.

2 METHODOLOGY

2.1 Thermodynamics Cycles

Until now, four possible thermodynamic cycles (P-h cycles) have been considered to achieve a higher discharge temperature of a transcritical CO_2 heat pump system, as shown in *Figs. 1 to 4*. Although all these cycles are theoretically achievable, they still need to be investigated considering industrial applicability. Theoretically, the simplest way to achieve a targeted discharge temperature (e.g. 180 °C) is to compress CO_2 vapour to a very high discharge pressure (e.g. 200 bar), as shown in *Fig. 1*. Then, the water heating process can be operated during the gas cooling process from state 2 to state 3. However, the high-pressurized CO_2 cycle is impractical in industry, due to the upper-pressure limit of compressors, e.g.140 bar is the maximum pressure of CO_2 compressors in Bitzer (which is a world-leading manufacturer of refrigeration compressors) (Bitzer 2019).

The second proposed thermodynamics cycle is to operate an auxiliary heating device, where the compressor reaches its maximum pressure, i.e. at around 140 bar. Then, the discharge temperature can be further increased from T_2 to $T_{2'}$, e.g. from 110°C to 180°C, as shown in *Fig. 2*. Although this scenario is practicable in industry, it relies more on auxiliary heater other than CO_2 heating, that is, considerable energy is required from the auxiliary input, leading to relatively low heating efficiency.

The third proposed cycle is to employ an IHX for transferring a part of rejection heat to superheat the suction CO_2 vapour (e.g. to around 45°C at state 1'), as shown in *Fig.3*. The targeted discharge temperature can be achieved at a lower discharge pressure after the compression process, compared to that of the second thermodynamics cycle. The advantages of this cycle include that: no more extra energy is required for the auxiliary heater and the efficiency can be improved by using an IHX. However, this scenario is still impractical due to the upper-temperature limit of available compressors. After several correspondences with experts at Bitzer in Germany, it has been told that the highest discharge temperature of compressors for the long-term is 140°C, although with only short events the system is able to operate above 140°C but not exceed 160°C. This is for limiting the low frequency of the compressor, as motor cooling is required with overly high superheat. Additionally, it was suggested that it is not sensible to go higher temperature through a compressor since even electric heating or gas heating would be more cost-efficient.

Therefore, the final thermodynamic cycle has been proposed by both using an IHX and operating an auxiliary heater, as shown in *Fig.4*. The system with an IHX is able to reach 140°C of the discharge temperature at relatively low pressure (e.g. 100 bar), followed by auxiliary heating of CO_2 to the targeted temperature. Based on this cycle, the CO_2 cycle operates within the temperature and pressure range of

the compressor. More importantly, the heating efficiency at such a low discharge pressure (which is near the critical point) is relatively high.

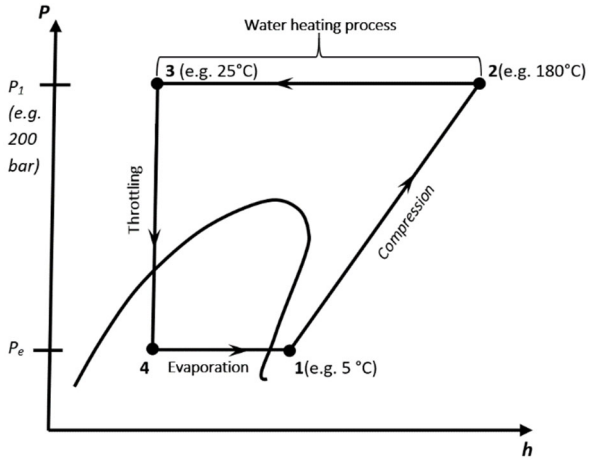

Fig. 1 The high-pressurized cycle of a CO_2 system

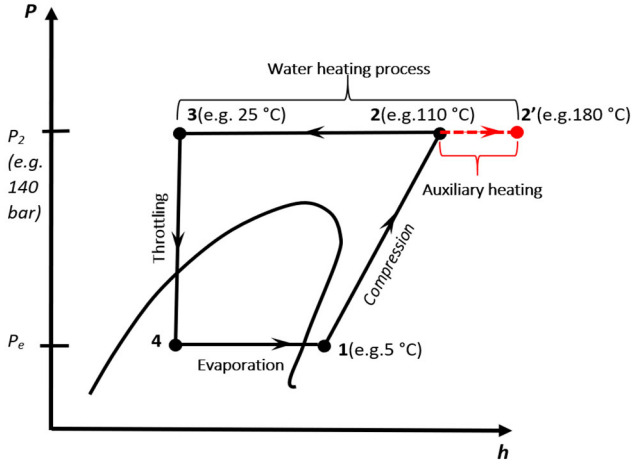

Fig. 2 The CO_2 cycle with an auxiliary heater

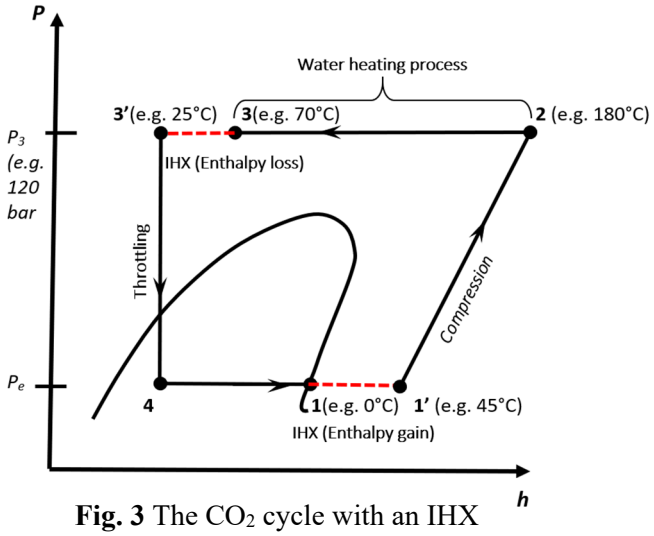

Fig. 3 The CO_2 cycle with an IHX

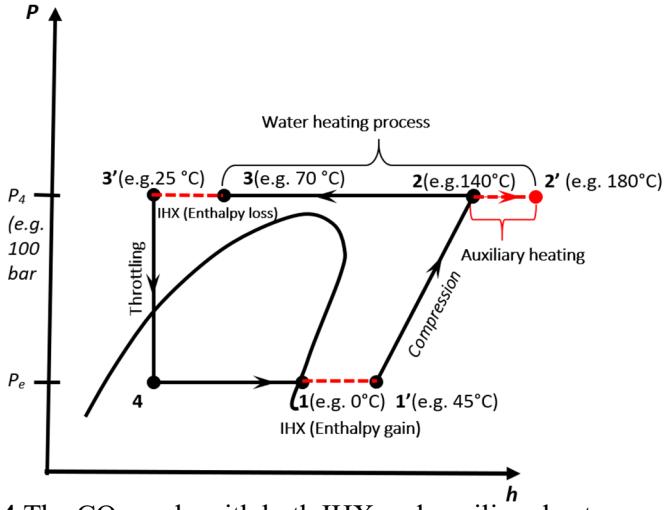

Fig. 4 The CO_2 cycle with both IHX and auxiliary heater

2.2 Physical Model

Due to the compressor constraints, the operating cycle with IHX and the auxiliary heater has been selected for boosting the discharge temperature, as shown in *Fig. 4*. In industry, due to a pressure regulator normally utilized with the compressor, the auxiliary heating process will be operated in an isobaric way. In terms of the amount of energy required, there is no difference in auxiliary heating of CO_2 or water in the system, of which working theories are described in *Fig. 5* and *Fig. 6* respectively. If the auxiliary heater is purposed for CO_2, the reheating process will occur followed by the compression in an isobaric process, in order to achieve a wider temperature range and larger heat capacity for delivery. Based on the existing counter-flow plate heat exchanger, the pinch temperature difference between water/steam and CO_2 can be minimized to 3K. However, if the process is for boosting water/ steam temperature directly, the auxiliary heating configuration will be set up after the heat exchanger process of the water loop.

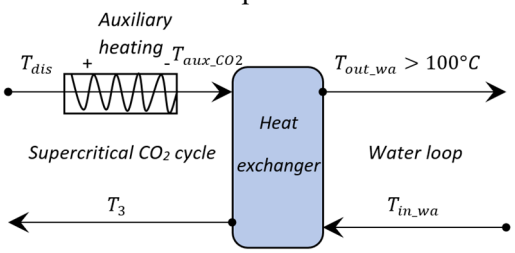

Fig. 5 The schematic of auxiliary CO_2 heating

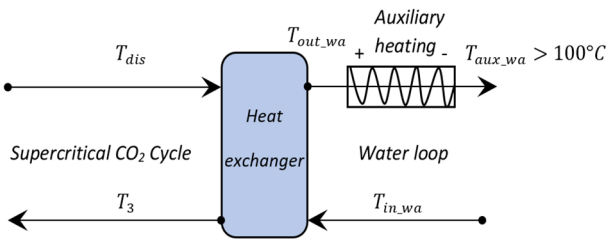

Fig. 6 The schematic of auxiliary water heating

In this study, the auxiliary heating process will aim at heating CO_2 rather than directly heating water due to three main reasons. Firstly, the cost regarding the configuration of heating CO_2 is cheaper than that of heating water. In industry, the components required for electric heating water include a boiler, heating elements and a control system (Schibel & Döring 2009). The heating elements are normally selected as Nichrome (Ni-Cr) coils inside a steel sheath surrounded by an insulator of magnesium oxide (MgO). Based on the whole configuration, the total cost of heating water is around \$0.15/W (Thermal 2019). However, in terms of heating CO_2, there is only a small tubular heating element required inside the pipe for boosting the discharge temperature. During the operation, the surface temperature of the heating element will be adjusted by the current which is controlled by a PID system. Therefore, the whole cost of heating CO_2 is expected to be lower than that of heating water directly. Moreover, sCO_2 with a higher temperature can generate a larger heat capacity, which can be utilised for multiple functions (Liu et al. 2017). It has been applied in some industries nowadays, e.g. magnetic media production, petrochemistry refinery, and food industry (Dadashev & Stepanov 2000; Johns 1998; Sarkar 2014). The properties of sCO_2 fluid are advantageous for some applications due to its larger compressibility and larger density compared to other gaseous substances, e.g. steam (Machida, Takesue & Smith 2011). Last but not least, auxiliary heating of CO_2 is a way to make the system integrated, which increases advances in automation and easier management. In the long run, system integration can lead to a promising application of the commercial product.

Additionally, the working principle of the IHX is to transfer a small part of rejection heat from the gas cooling process to superheat the suction CO_2 vapour before compression, (e.g. heating suction vapour to around 45°C at state 1'). The working theory of the IHX is described in *Fig. 7*.

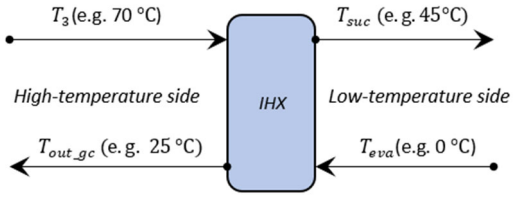

Fig. 7 The working theory of the IHX in a CO_2 system

2.3 Mathematical Model

The mathematical model of a transcritical CO_2 heat pump with the auxiliary heater has been developed in this section. Several typical assumptions have been made as follows:

1. The system operates at a steady state.
2. The compression work is an adiabatic but not an isentropic process.
3. Pressure drop during the gas cooling process is negligible.
4. There is no lubricant oil left during the gas cooling process, post-compression.
5. Heat loss in the resistance heating wires during the auxiliary heating is negligible.

Heat capacity in a CO_2 system with the auxiliary heater is comprised of two parts, i.e. the original heat capacity generated by the compressor (Q_{gc_ori}) and the extra heat capacity due to the auxiliary heating process (Q_{aux}), which can be described as:

$$Q_{heat} = Q_{gc\_ori} + Q_{aux} \tag{1}$$

$$Q_{gc\_ori} = \dot{m} \times (h_{gc\_in\_ori} - h_{gc\_out}) \tag{2}$$

$$Q_{aux} = \dot{m} \times (h_{gc\_in} - h_{gc\_in\_ori}) \tag{3}$$

where $\dot{m}$ is the mass flow rate of the refrigerant, $h_{gc\_in\_ori}$ is the enthalpy at the original inlet of the gas cooler without the auxiliary heater, h_{gc_in} is the refrigerant enthalpy at the inlet of the gas cooler with auxiliary heater, and h_{gc_out} is the enthalpy at the outlet of the gas cooler. Due to that, an auxiliary heater is set up after the compressor and a pressure regulator is normally utilized with the compressor, hence the mass flow rate of the refrigerant keeps constant during the heating process.

Heating efficiency is the ratio of total heat capacity over the energy input (including compression work and auxiliary energy supply), which can be described as:

$$\eta_{heat} = Q_{heat}/(W_{comp} + Q_{aux}) \quad (4)$$

where W_{comp} is the compression work.

- **CO_2 Compressor**

The mass flow rate of a single semi-hermetic reciprocating compressor can be defined as (Wang et al. 2021):

$$\dot{m}_{comp} = \frac{\eta_v \times V_s}{v_{suc}} \quad (5)$$

where η_v is the volumetric efficiency of the compressor, v_{suc} is the specific volume of CO_2 at the compressor suction state, which depends on the suction gas superheat ΔT_{super} and the evaporation temperature T_{eva}, and V_s is the displacement rate of the compressor.

In terms of compressor performance, the compression ratio is defined as the discharge pressure (P_{dis}) over the suction pressure (P_{suc}), that is：

$$r = \frac{P_{dis}}{P_{suc}} \quad (6)$$

In this study, the volumetric efficiency for a semi-hermetic compressor manufactured from Bitzer can be estimated with the function of compression ratio (Bitzer 2019), of which correlation is:

$$\eta_v = 1.1785 - 0.1755 \times r + 0.0152 \times r^2 \quad (7)$$
$$R^2 = 0.9999$$

The isentropic efficiency of a Bitzer compressor can be estimated with real performance data. Hence, when the compression ratio is below 3, the correlation is:

$$\eta_{isentr1} = -161.48 + 413.74r - 438.47r^2 + 247.09r^3 - 78.081r^4 + 13.117r^5 - 0.915r^6 \quad (8)$$
$$R^2 = 0.9952$$

When the compression ratio is over 3, then the correlation is:

$$\eta_{isentr2} = 0.192 + 0.6443r - 0.2813r^2 + 0.0517r^3 - 0.0035r^4 \quad (9)$$
$$R^2 = 0.9944$$

Therefore, the energy required for compression work can be calculated from:

$$W_{comp} = \frac{\dot{m}_{comp}(h_{dis,isentr} - h_{suc})}{\eta_{isentr}} \quad (10)$$

where $h_{dis,isentr}$ is a specific enthalpy at the discharge state during an isentropic compression process and h_{suc} is the specific enthalpy at the compressor suction state.

Then, the enthalpy at the discharge state post-compression can be calculated from:

$$h_{dis} = h_{suc} + \frac{W_{comp}}{\dot{m}_{comp}} \quad (11)$$

For a single compressor, the discharge temperature T_{dis} can be worked out once the enthalpy and pressure at the discharge state have been known. The equations with constants for calculating the CO_2 property has been derived by Huang et al. and simplified by Span and Wagner (Huang et al. 1985), (Span & Wagner 1996).

3 PRELIMINARY VALIDATION

The mathematical model of a semi-hermetic reciprocating compressor has been validated against the experimental data recorded from an existing installation, as shown in *Appendix*. The system operated with the arrangement of parallel compression, in which compressor 1 worked as a main compressor and compressor 2 operated as an auxiliary compressor. The technical data for the compressor (Type: 4HTE-20K) used in the system at 50Hz is given as the displacement rate is 12 m^3/h. Compressor 1 operated with the VSD ranging from 30 to 60 Hz, while compressor 2 operated with an FSD of 50 Hz. The power consumption for a compressor changed with conditions at the suction and discharge states.

The predicted and actual power consumptions for compressor 1 with VSD and compressor 2 with FSD are displayed in *Fig.8*. In terms of the compressor with VSD, the results show an acceptable agreement with most errors within ±10%. But the simulation has the highest errors when the system is warming up, i.e. the actual power consumption is below 6 kW. However, for the FSD compressor, the difference between the predicted power and the actual power is within ±5%, which is more accurate

than that of the compressor with the VSD. It can be explained that compressor 1 with the inverters adjusted the frequency constantly, while compressor 2 always ran at a fixed frequency. Overall, the simulation can predict the power consumption for both FSD and VSD compressors with reasonable uncertainties.

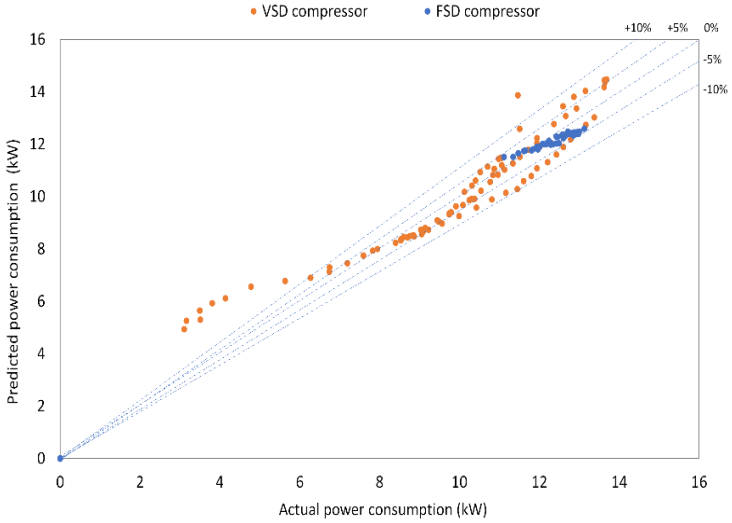

Fig. 8 Predicted and measured compressor power consumption

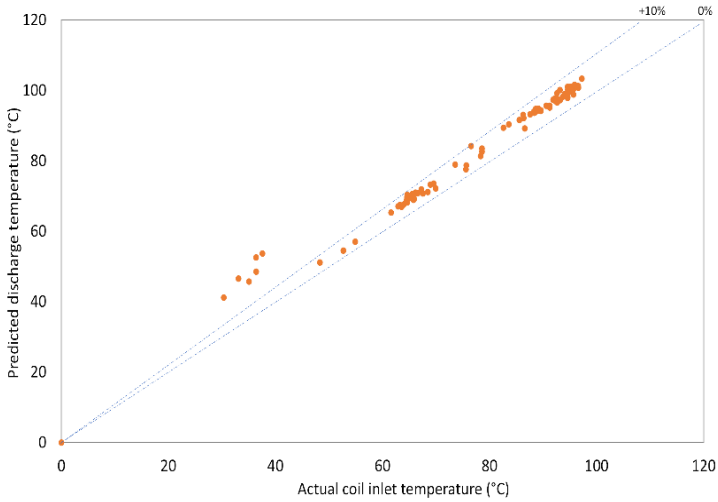

Fig. 9 Predicted and measured temperatures

The predicted discharge temperatures and the measured coil inlet temperatures have also been compared, as described in *Fig. 9*. It shows that the predicted results are always higher than the actual ones with an error of less than 10%; even the highest errors occur when the system is warming up in the first few minutes. Theoretically, the discharge temperature post-compression is supposed to be the same as the coil inlet temperature. However, in practice, the coils are installed a certain distance apart from the compressor, so it will have some energy losses during the sCO_2 transportation process when the ambient condition is cold, even with the pipes around the heating coils have been relatively well-insulated (Bojić, Miletić & Bojić 2014).

4 SIMULATION RESULTS

The numerical analysis for a transcritical CO_2 heat pump with the auxiliary heater has been carried out. Several preliminary results with different discharge pressures are described in this section. Several known conditions have been given in *Table 1*. The maximum temperature and pressure of the compressor are 140 °C and 140 bar respectively. The targeted discharge temperature of CO_2 is set as 180 °C when the ambient water (that is, approximately 20°C at the inlet) needs to be heated up higher than 100°C.

Table 1 Known conditions for a transcritical CO_2 heat pump with IHX and the auxiliary heater

T_eva	0	°C
T_out_IHX	25	°C
P_suc	34.851	bar
ΔT_suc	25	K
T_target	180	°C
Compressor	4HTE-20K-50Hz	
Upper pressure limit	140	bar
Upper temperature limit	140	°C

The results shown in *Table 2* gives the heating performance with the increase of discharge pressure from 75 bar to 110 bar. When the superheat is 25K and the outlet temperature of IHX is 25°C, the inlet temperature of IHX depends on the CO_2 properties at different discharge pressures. It can be seen that the highest discharge temperature at the pressure of 110 bar is 139.300 °C. Due to that, the maximum temperature of the compressor has been reached around 110 bar, hence, the heating performance with higher pressure is not necessarily to be studied.

Table 2 The calculated results with the increase of pressure from 75 bar to 110 bar

Pressures (bar)	75	80	85	90	95	100	105	110	115
Compression ratio	2.152	2.295	2.439	2.582	2.726	2.869	3.013	3.156	
Mass flow rate (kg/s)	0.225	0.221	0.218	0.214	0.211	0.207	0.204	0.201	
IHX inlet temperature (°C)	31.025	32.445	33.565	34.487	35.265	35.939	36.529	37.057	
Discharge temperature (°C)	96.700	103.400	109.800	116.000	122.100	128.000	133.700	139.300	144.800
Compressor Input (kW)	11.580	12.490	13.350	14.170	14.950	15.700	16.410	17.090	
Original heat capacity (kW)	48.778	49.5858	50.30993	50.871	51.42	51.806	52.242	52.618	
Auxiliary heater (kW)	22.385	20.4226	18.59625	16.826	15.114	13.457	11.899	10.384	
Auxiliary heat capacity (kW)	22.385	20.4226	18.59625	16.826	15.114	13.457	11.899	10.384	
COP without auxiliary heater	4.212	3.970	3.769	3.590	3.439	3.300	3.184	3.079	
COP with auxiliary heater	2.095	2.127	2.157	2.184	2.213	2.238	2.266	2.293	

Then, the COP variation and discharge temperature with the increase of pressure is displayed in *Fig. 10*. The discharge temperature increases significantly with the pressure, while the COP without the auxiliary heater reduces with the pressure. However, if the CO_2 heating process is combined with the auxiliary heater, the total heating COP increases slightly with the discharge pressure.

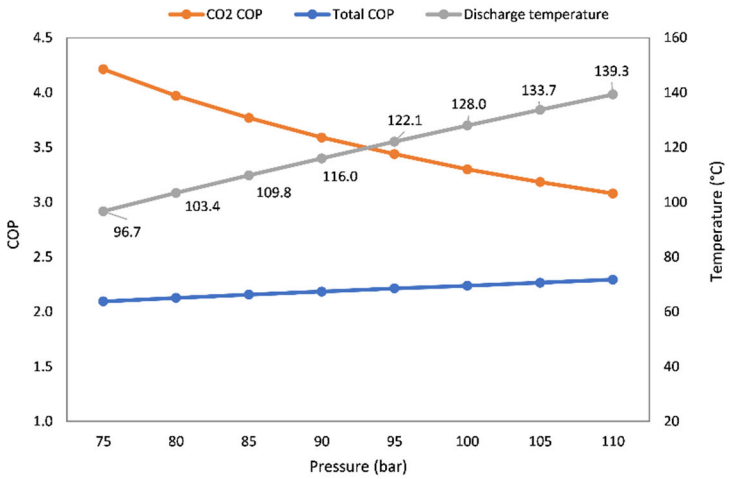

Fig. 10 COP and discharge gas temperature Vs. pressure

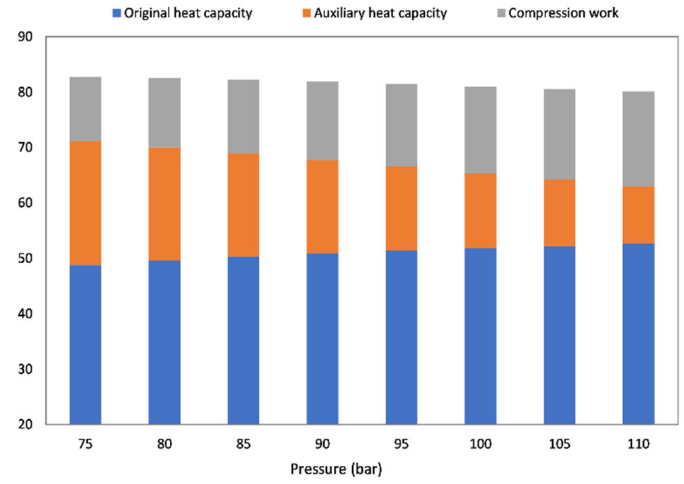

Fig. 11 Energy distribution with the increased pressure

In terms of the energy distribution, as shown in *Fig.11*, the ratio of auxiliary heat capacity to CO_2 heat capacity reduces with the increase of pressure, although the compressor input keeps increasing with the discharge pressure. Therefore, it is meaningful to operate an auxiliary heater at an optimal discharge pressure to achieve the maximum heating COP with a targeted discharge temperature of CO_2.

5 CONCLUSION

The following conclusions can be drawn from this preliminary study on a transcritical CO_2 high-temperature heat pump:

- Four thermodynamic cycles have been identified and investigated with the consideration of industrial applicability. Based on the selected cycle, the physical model of the auxiliary heater has been developed.
- The mathematical model for Bitzer compressors with VSD and FSD has been validated against the existing experimental data, in which the simulated errors for both compressors are within ± 10%. The discharge temperatures have also been validated against the actual coil inlet temperatures with acceptable agreements.
- The mathematical model of the heating performance for a transcritical CO_2 system with the auxiliary heater has been established. The simulation result shows that the total efficiency of the system does not have an obvious change in COPs (from 2 to 2.3) with various discharge temperatures by increasing the discharge pressure, which can be used to justify the auxiliary heater in a transcritical CO_2 heat pump.

NOMENCLATURE

Cp	specific heat capacity, kJ/kg.K	GWP	Global Warming Potential
D	diameter of the bore inside the cylinder, m	HCFC	Hydrochlorofluorocarbon
h	enthalpy, kJ/kg	HFC	Hydrofluorocarbons
$\dot{m}$	mass flow rate, kg/s	IHX	Internal Heat Exchanger
P	pressure, bar	ODP	Ozone Depletion Potential
Q	heating power, kW	PID	Proportional Integral Derivative
r	compresssion ratio	RPM	Revolution Per Minute
R^2	R-Squared value	sCO_2	Supercritical CO_2
t	time, seconds	VSD	Variable Speed Drive
T	temperature, °C	***Subscripts***	
ΔT	temperature difference, K or °C	aux	auxiliary
$\dot{V}$	volumetric flow rate, m^3/s	comp	compressor
V_s	displacement rate of the compressor, m^3/s	dis	discharge
W_{comp}	compression work, kW	eva	evaporation
Greek symbols		gc	gas cooler
η	efficiency	heat	heating
η_v	volumetric efficiency of a CO_2 compressor	in	inlet
v	specific volume, m^3/kg	isentr	isentropic
Abbreviations		ori	original
AHU	Air Handling Unit	out	outlet
CFC	Chlorofluorocarbon	suc	suction
COP	Coefficient of Performance	super	superheat
FG	Flash-Gas	wa	water
FSD	Fixed Speed Drive	1 to 4	refrigerants states

REFERENCES

Bamigbetan, O, Eikevik, TM, Nekså, P & Bantle, M 2017, 'Review of vapour compression heat pumps for high temperature heating using natural working fluids', *International Journal of Refrigeration,* vol. 80, 2017/08/01/, pp. 197-211.

Bitzer 2019, *Bitzer online software*, <https://www.bitzer.de/websoftware/Calculate.aspx?cid=1576028948781&mod=HHK>.

Bojić, M, Miletić, M & Bojić, L 2014, 'Optimization of thermal insulation to achieve energy savings in low energy house (refurbishment)', *Energy Conversion and Management,* vol. 84, 2014/08/01/, pp. 681-90.

Bruno, F, Belusko, M & Halawa, E 2019, 'CO2 Refrigeration and Heat Pump Systems—A Comprehensive Review', *Energies,* vol. 12, no. 15, p. 2959.

Chaichana, C, Aye, L & Charters, WWS 2003, 'Natural working fluids for solar-boosted heat pumps', *International Journal of Refrigeration,* vol. 26, no. 6, 2003/09/01/, pp. 637-43.

Chris Riedy, GM, Paul Ryan 2013, *Hot water service*, <https://www.yourhome.gov.au/energy/hot-water-service>.

Dadashev, MN & Stepanov, GV 2000, 'Supercritical extraction in petroleum refining and petrochemistry', *Chemistry and Technology of Fuels and Oils,* vol. 36, no. 1, pp. 8-13.

Hepbasli, A & Kalinci, Y 2009, 'A review of heat pump water heating systems', *Renewable and Sustainable Energy Reviews,* vol. 13, no. 6, 2009/08/01/, pp. 1211-29.

Huang, F-H, Li, M-H, Lee, LL, Starling, KE & Chung, FTH 1985, 'AN ACCURATE EQUATION OF STATE FOR CARBON DIOXIDE', *Journal of Chemical Engineering of Japan,* vol. 18, no. 6, pp. 490-96.

Johns, K 1998, 'Supercritical fluids—a novel approach to magnetic media production?: An introduction to supercritical fluid technologies and how they might be applied to deposition/impregnation of

metallics, magnetic inks and protective lubrication', *Tribology International,* vol. 31, no. 9, 1998/09/01/, pp. 485-90.

Kim, M-H, Pettersen, J & Bullard, CW 2004, 'Fundamental process and system design issues in CO2 vapor compression systems', *Progress in Energy and Combustion Science,* vol. 30, no. 2, 2004/01/01/, pp. 119-74.

Kus, B & Nekså, P 2013, 'Oil free turbo-compressors for CO2 refrigeration applications', *International Journal of Refrigeration,* vol. 36, no. 5, 2013/08/01/, pp. 1576-83.

Liu, Y, Groll, EA, Yazawa, K & Kurtulus, O 2017, 'Energy-saving performance and economics of CO2 and NH3 heat pumps with simultaneous cooling and heating applications in food processing: Case studies', *International Journal of Refrigeration,* vol. 73, 2017/01/01/, pp. 111-24.

Lorentzen, G 1994, 'Revival of carbon dioxide as a refrigerant', *International Journal of Refrigeration,* vol. 17, no. 5, 1994/01/01/, pp. 292-301.

Machida, H, Takesue, M & Smith, RL 2011, 'Green chemical processes with supercritical fluids: Properties, materials, separations and energy', *The Journal of Supercritical Fluids,* vol. 60, 2011/12/01/, pp. 2-15.

Maina, P & Huan, Z 2015, 'A review of carbon dioxide as a refrigerant in refrigeration technology', *South African Journal of Science,* vol. 111, pp. 01-10.

Nekså, P 2002, 'CO2 heat pump systems', *International Journal of Refrigeration,* vol. 25, no. 4, pp. 421-27.

Nellissen, P & Wolf, S 2015, 'Heat pumps in non-domestic applications in Europe: potential for an energy revolution', *Emerson Climate Technologies, Delta-ee 3rd Annual Heat Pumps & Utilities Roundtable*.

Qi, P-C, He, Y-L, Wang, X-L & Meng, X-Z 2013, 'Experimental investigation of the optimal heat rejection pressure for a transcritical CO2 heat pump water heater', *Applied Thermal Engineering,* vol. 56, no. 1, 2013/07/01/, pp. 120-25.

Saikawa, M & Koyama, S 2016, 'Thermodynamic analysis of vapor compression heat pump cycle for tap water heating and development of CO2 heat pump water heater for residential use', *Applied Thermal Engineering,* vol. 106, 2016/08/05/, pp. 1236-43.

Sarkar, J 2014, 'On suitability of supercritical carbon dioxide as heat transfer fluid in flat plate solar collector', *Journal of Thermal Engineering & Applications,* vol. 1, 01/01, pp. 1-9.

Schibel, T & Döring, H 2009, 'Energy-efficient steam generation with industrial/commercial boiler systems', *Gaswaerme International,* vol. 58, no. 1-2, pp. 48-53.

Span, R & Wagner, W 1996, 'A New Equation of State for Carbon Dioxide Covering the Fluid Region from the Triple-Point Temperature to 1100 K at Pressures up to 800 MPa', *Journal of Physical and Chemical Reference Data,* vol. 25, no. 6, 1996/11/01, pp. 1509-96.

Stene, J 2005, 'Residential CO2 heat pump system for combined space heating and hot water heating', *International Journal of Refrigeration,* vol. 28, no. 8, 2005/12/01/, pp. 1259-65.

Tammaro, M, Montagud, C, Corberán, JM, Mauro, AW & Mastrullo, R 2017, 'Seasonal performance assessment of sanitary hot water production systems using propane and CO2 heat pumps', *International Journal of Refrigeration,* vol. 74, 2017/02/01/, pp. 224-39.

Thermal 2019, *Industrial Heating*, viewed 15/Feb, <https://www.thermalproducts.com.au/industrial-heating/>.

Velders, GJM, Andersen, SO, Daniel, JS, Fahey, DW & McFarland, M 2007, 'The importance of the Montreal Protocol in protecting climate', *Proceedings of the National Academy of Sciences,* vol. 104, no. 12, pp. 4814-19.

Wang, J, Belusko, M, Liu, M, Semsarilar, H, Liddle, R, Alemu, A, Evans, M, Zhao, C, Hudson, J & Bruno, F 2021, 'A comprehensive study on a novel transcritical CO2 heat pump for simultaneous space heating and cooling – Concepts and initial performance', *Energy Conversion and Management,* vol. 243, 2021/09/01/, p. 114397.

White, SD, Yarrall, MG, Cleland, D & Hedley, R 2002, 'Modelling the performance of a transcritical CO2 heat pump for high temperature heating (Reprinted)', *Int. J. Refrig.-Rev. Int. Froid,* vol. 25, no. 4, pp. 479-86.

Zheng, S, Wei, M, Song, P, Hu, C & Tian, R 2020, 'Thermodynamics and flow unsteadiness analysis of trans-critical CO2 in a scroll compressor for mobile heat pump air-conditioning system', *Applied Thermal Engineering,* vol. 175, 2020/07/05/, p. 115368.

ACKNOWLEDGEMENT

The authors would like to acknowledge the Australian Government for the Research Training Program (RTP) scholarship. The authors would also like to thank Glaciem Cooling Technologies for their industrial support and the resources provided.

APPENDIX

TIME	COMP_1(KW)	COMP_1 (Hz)	COMP_2 (KW)	COMP_2 (Hz)	MT_COMP_SUCT_PRESS (Kpa)	COMPS_DISC_PRESS (kPa)	MT_COMP_SUCT_TEMP (°C)	COIL_HEAT_SUPPLY_TEMP (°C)	COIL_HEAT_RETURN_TEMP (°C)
9:07:00 AM	0.00	30.00	0.00	0.00	2657.81	5692.03	0.00	30.33	20.08
9:07:30 AM	3.51	30.00	0.00	0.00	3389.91	5520.94	2.89	33.08	19.73
9:08:00 AM	3.11	31.00	0.00	0.00	3548.34	5340.47	8.33	35.04	19.98
9:08:30 AM	3.16	32.00	0.00	0.00	3573.66	5332.73	10.65	36.39	19.22
9:09:00 AM	3.50	33.00	0.00	0.00	3551.53	5387.34	11.70	36.36	18.58
9:09:30 AM	3.81	34.00	0.00	0.00	3525.94	5414.06	12.14	37.54	18.89
9:10:00 AM	4.14	35.00	0.00	0.00	3549.56	5507.81	12.38	52.68	18.89
9:10:30 AM	4.78	36.00	0.00	0.00	3543.09	5716.17	12.50	48.29	19.33
9:11:00 AM	5.64	37.00	0.00	0.00	3544.31	6018.52	12.54	54.90	20.38
9:11:30 AM	6.75	38.00	0.00	0.00	3546.19	6431.95	12.59	61.59	22.13
9:12:00 AM	7.83	39.00	0.00	0.00	3500.25	6746.72	12.67	67.53	23.06
9:12:30 AM	8.53	40.00	0.00	0.00	3444.94	6854.53	12.53	69.54	23.16
9:13:00 AM	8.85	41.00	0.00	0.00	3453.09	6851.48	12.50	68.93	23.15
9:13:30 AM	9.09	42.00	0.00	0.00	3469.88	6806.25	12.50	69.93	22.17
9:14:00 AM	9.05	43.00	0.00	0.00	3473.06	6621.56	12.42	65.14	22.16
9:14:30 AM	9.22	44.00	0.00	0.00	3480.00	6604.45	12.38	65.86	22.19
9:15:00 AM	9.56	45.00	0.00	0.00	3496.50	6632.58	12.38	65.76	22.16
9:15:30 AM	9.99	46.00	0.00	0.00	3508.69	6690.47	12.38	65.86	21.86
9:16:00 AM	10.42	47.00	0.00	0.00	3508.69	6757.73	12.38	65.58	23.31
9:16:30 AM	10.81	48.00	0.00	0.00	3513.09	6821.72	12.37	66.15	23.20
9:17:00 AM	11.16	49.00	0.00	0.00	3517.41	6849.84	12.29	68.45	22.83
9:17:30 AM	11.45	50.00	0.00	0.00	3600.84	6841.17	12.39	64.52	22.91
9:18:00 AM	11.60	51.00	0.00	0.00	3651.19	6913.83	11.60	63.25	23.15
9:18:30 AM	11.80	52.00	0.00	0.00	3668.72	6905.39	11.61	63.56	24.27
9:19:00 AM	11.94	53.00	0.00	0.00	3695.53	6962.34	11.73	62.90	24.43
9:19:30 AM	12.21	54.00	0.00	0.00	3701.81	6978.05	12.16	63.99	24.36
9:20:00 AM	12.43	55.00	0.00	0.00	3711.19	7020.23	12.36	64.60	24.41
9:20:30 AM	12.60	56.00	0.00	0.00	3700.59	7057.73	12.50	65.86	24.37
9:21:00 AM	12.79	57.00	0.00	0.00	3697.50	7090.55	12.46	65.26	24.11
9:21:30 AM	12.92	58.00	0.00	0.00	3703.03	7117.03	12.41	64.56	23.94
9:22:00 AM	13.16	59.00	0.00	0.00	3705.56	7149.84	12.41	65.24	24.10
9:22:30 AM	13.37	60.00	0.00	0.00	3706.22	7185.94	12.32	64.59	24.29
9:23:00 AM	6.27	30.00	11.51	50.00	3535.59	7491.33	12.15	75.64	25.30
9:23:30 AM	6.74	31.00	11.52	50.00	3430.59	7481.25	11.95	78.33	24.97
9:24:00 AM	7.19	32.00	11.65	50.00	3413.72	7566.09	11.73	78.56	23.96
9:24:30 AM	7.59	33.00	11.74	50.00	3396.47	7625.63	11.44	78.56	23.99
9:25:00 AM	7.95	34.00	11.76	50.00	3374.06	7643.67	11.31	76.54	23.95
9:25:30 AM	8.40	35.00	11.76	50.00	3234.00	7679.53	11.74	82.59	24.08
9:26:00 AM	8.76	36.00	11.80	50.00	3237.09	7706.02	12.29	83.59	24.46
9:26:30 AM	9.14	37.00	11.89	50.00	3228.00	7770.94	12.42	85.57	24.44
9:27:00 AM	9.48	38.00	11.91	50.00	3218.63	7790.63	12.42	86.36	24.41
9:27:30 AM	9.75	39.00	12.00	50.00	3217.50	7867.03	12.42	86.25	24.41
9:28:00 AM	9.91	40.00	12.03	50.00	3198.66	7907.81	12.58	89.26	24.41
9:28:30 AM	10.25	41.00	12.03	50.00	3184.69	7913.91	12.51	88.57	24.39
9:29:00 AM	10.38	42.00	11.80	50.00	3166.22	7737.42	12.50	87.56	23.42
9:29:30 AM	10.54	43.00	11.89	50.00	3168.66	7803.05	12.51	88.23	24.42
9:30:00 AM	10.77	44.00	12.00	50.00	3154.31	7913.91	12.51	90.56	24.49
9:30:30 AM	10.97	45.00	12.04	50.00	3123.75	7982.58	12.51	92.36	25.57
9:31:00 AM	11.13	46.00	11.98	50.00	3098.63	7958.44	12.51	94.57	25.46
9:31:30 AM	11.34	47.00	11.99	50.00	3079.03	7990.55	12.51	95.66	25.54
9:32:00 AM	11.51	48.00	11.99	50.00	3071.81	8009.06	12.47	92.57	25.56
9:32:30 AM	11.72	49.00	12.02	50.00	3058.69	8060.86	12.42	93.14	25.52
9:33:00 AM	11.94	50.00	12.04	50.00	3045.56	8114.06	12.41	94.57	25.48
9:33:30 AM	11.94	51.00	11.99	50.00	3190.22	7882.03	12.29	88.57	25.50
9:34:00 AM	12.36	52.00	12.27	50.00	3212.44	8104.45	11.58	89.12	26.61
9:34:30 AM	12.66	53.00	12.33	50.00	3186.47	8187.42	10.90	91.24	26.57
9:35:00 AM	12.93	54.00	12.38	50.00	3169.31	8266.88	10.85	92.35	26.57
9:35:30 AM	12.59	55.00	12.23	50.00	3125.63	8168.67	10.89	93.15	26.59
9:36:00 AM	12.86	56.00	12.33	50.00	3154.97	8228.67	10.89	92.85	26.53
9:36:30 AM	13.15	57.00	12.31	50.00	3127.50	8257.73	10.89	94.57	27.48
9:37:00 AM	13.62	58.00	12.45	50.00	3137.44	8406.80	10.96	94.77	28.87
9:37:30 AM	13.68	58.00	12.47	50.00	3133.69	8449.92	10.98	94.86	29.58
9:38:00 AM	13.64	58.00	12.39	50.00	3100.22	8426.48	10.98	96.56	29.65
9:38:30 AM	13.62	57.00	12.44	50.00	3116.81	8459.06	10.85	95.69	31.08
9:39:00 AM	11.06	45.00	12.44	50.00	3167.44	8332.73	10.85	92.15	31.13
9:39:30 AM	8.87	34.00	12.47	50.00	3252.09	8256.09	10.89	89.56	31.05
9:40:00 AM	8.61	34.00	12.44	50.00	3190.59	8295.00	11.64	92.56	29.33
9:40:30 AM	8.54	34.00	12.32	50.00	3183.00	8185.08	12.15	91.87	28.83
9:41:00 AM	8.70	35.00	12.06	50.00	3201.84	7926.33	12.38	89.56	26.56
9:41:30 AM	9.03	36.00	12.12	50.00	3233.06	7957.03	12.42	88.34	26.63
9:42:00 AM	9.44	37.00	12.29	50.00	3235.22	8098.13	12.41	91.23	26.58
9:42:30 AM	9.79	38.00	12.37	50.00	3221.81	8188.83	12.42	92.63	26.13
9:43:00 AM	10.09	39.00	12.40	50.00	3193.03	8256.09	12.42	93.65	27.26
9:43:30 AM	10.30	40.00	12.39	50.00	3171.19	8267.11	12.41	94.02	27.64
9:44:00 AM	10.12	41.00	12.41	50.00	3157.13	8326.41	12.51	95.24	27.79
9:44:30 AM	10.31	42.00	12.41	50.00	3136.13	8356.88	12.51	96.25	27.81
9:45:00 AM	10.40	43.00	12.33	50.00	3132.19	8277.19	12.42	94.61	26.68
9:45:30 AM	10.52	44.00	12.42	50.00	3138.09	8368.59	12.42	95.12	28.84
9:46:00 AM	10.70	45.00	12.38	50.00	3122.44	8352.19	12.37	96.56	28.31
9:46:30 AM	11.03	46.00	12.48	50.00	3107.16	8530.31	12.30	97.23	30.20
9:47:00 AM	9.74	37.00	12.59	50.00	3171.19	8515.31	12.51	95.89	33.29
9:47:30 AM	11.46	57.00	0.00	50.00	3375.56	7920.94	12.65	86.56	32.60
9:48:00 AM	11.07	50.00	0.00	50.00	3564.28	7485.94	13.02	73.56	30.25
9:48:30 AM	10.84	50.00	0.00	50.00	3685.88	7164.84	13.31	67.23	27.66
9:49:00 AM	10.87	51.00	0.00	50.00	3758.06	7195.08	13.46	65.56	28.31
9:49:30 AM	10.98	52.00	0.00	50.00	3798.09	7298.20	13.48	66.57	28.81
9:50:00 AM	11.51	53.00	0.00	50.00	3759.00	7756.88	13.60	75.57	29.62
9:50:30 AM	12.01	53.00	0.00	50.00	2883.00	7491.09	12.88	94.69	30.17
9:51:00 AM	0.00	30.00	0.00	50.00	2323.69	7009.22	10.79	60.90	29.54